

# Energy Performance of Membrane Energy Recovery Ventilation in Combination with an Exhaust Air Heat Pump

Fabian Ochs<sup>1</sup>, Martin Hauer<sup>1</sup>, Michele Bianchi Janetti<sup>1</sup>, Siegele Dietmar<sup>1</sup>

<sup>1</sup>University of Innsbruck, Unit for Energy Efficient Buildings, Innsbruck

## Abstract

Since the first discussion on energy recovery ventilation (ERV) in the literature some years ago, several papers were published about thermal comfort, performance and ERV modelling. However, a combination of membrane ERV and exhaust air heat pump (such as in a Passive House compact unit for ventilation, heating and DHW preparation) was not discussed in any of the previous studies. In an exhaust air heat pump, the exhaust air is the source of the heat pump and its performance is directly connected to the effectiveness of the ERV. The effectiveness of the ERV depends on the operation and boundary conditions (in particular the average relative humidity and the volume flow). Both are strongly coupled to the building and its use and operation. By means of simulation the complex dependencies are investigated. Simulation models for ERV are developed and compared against experimental data from the literature. For equal indoor air relative humidity, the air exchange rate can be significantly increased with ERV compared to a heat recovery ventilation (HRV). This will lead to a further improvement of the indoor air quality and to a significant better of the performance of the heat pump and an increase of the heating capacity.

## Introduction

Air-to-air membrane energy recovery ventilation (ERV) is increasingly discussed as a solution in residential buildings for reducing the energy consumed for heating and cooling as well as for improving the indoor air quality by dehumidifying or humidifying the ventilation air. Membrane based total energy (or so-called enthalpy) exchangers allow for simultaneous heat and moisture transfer through a selectively permeable membrane. In cold climates, the problem of dry air in winter may be reduced and frosting may be prevented or at least reduced when the exhaust air is sufficiently dry after the moisture recovery. However, there is the disadvantage of significantly higher investment costs for a membrane ERV compared to a heat recovery ventilation (HRV). In addition, there is an increased risk of mould growth in transition times (spring, autumn) or when applied in new buildings with high construction moisture content.

In combination with exhaust air heat pumps, ERV seems to be a very promising solution. Usually the specific heating power is limited to approx. 10 W/m<sup>2</sup> in such heating systems as the specific heating power is coupled to the hygienic flow rate (assuming 20 to 30 m<sup>3</sup>/h/P and a average occupation density of 30 m<sup>2</sup>/P). Excessive flow rates should be avoided in order to prevent too dry air, in particular in cold climates. Higher volume flows can be

realized with ERV compared to HRV without violating the lower limit for the indoor relative humidity (rH).

## Review of ERV

Energy Recovery Ventilation ERV was proposed by some authors e.g. by Schnieders et al. (2008) or Zhang et al. (2010) already several years ago and since then quite some work was done, as can be seen in the review papers that were recently published, see e.g. Alonso et al. (2015).

In the Passive House (PH) component data base (database.passivehouse.com, Nov. 2016) there are 19 certified units with moisture recovery. It can be clearly seen in Fig. 1 that the heat recovery (HR) effectiveness is correlated (by NTU as function of the heat exchanger area  $A_{HX}$ ) to the moisture recovery (MR) effectiveness, however, it can also be recognized that for a given heat recovery effectiveness, e.g. 85 %, the moisture recovery effectiveness can vary between 47 % and 77 % which can be explained either by different membrane properties (i.e. the equivalent air layer thickness  $s_d$  or water vapour diffusion resistance factor  $\mu$ , respectively) and/or by different operation conditions.

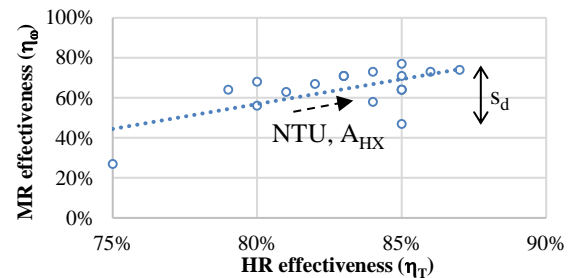


Figure 1: Moisture recovery (MR) vs. heat recovery (HR) effectiveness of certified ventilation units (passiv.de); influence of area  $A_{HX}$  and the equivalent air layer thickness  $s_d$

In Fig. 1, the (dry) heat recovery (or sensible) effectiveness is measured with mass balanced flows and is given acc. to the definition of the Passive House Institute (PHI, www.passiv.de)

$$\eta_{PHI} = \frac{(\vartheta_{ext} - \vartheta_{exh}) + P_{el}/\dot{m} \cdot c_p}{\vartheta_{ext} - \vartheta_{amb}} \quad (1)$$

The term  $P_{el}/\dot{m} \cdot c_p$  is included in the temperature ( $\vartheta$ ) effectiveness to account for the correct use in the energy balance (as required in the PHPP, passive.de)

The moisture recovery (or latent) effectiveness is measured under the following conditions:

- Extract air: 21 °C, 50 %,
- Ambient air: 4 °C, 80 %

and is defined as follows:

$$\eta_{\omega} = \frac{\omega_{ext} - \omega_{exh}}{\omega_{ext} - \omega_{amb}} \quad (2)$$

with the humidity ratio  $\omega$ . For the energy balance calculation within the PHPP the declared heat recovery effectiveness (PHI definition) is increased according to

$$\eta_{PHI,declared} = \eta_{PHI} + \min(0.048; \eta_{\omega} \cdot 0.08) \quad (3)$$

in order to account for the influence on the moisture balance (e.g. moisture buffer of walls) and the enhanced enthalpy transfer in case of ERV compared to HRV.

Flow rates of mechanical ventilation with heat recovery (MVHR) units reported on (www.passiv.de, < 600 m<sup>3</sup>/h) vary from 60 m<sup>3</sup>/h to 460 m<sup>3</sup>/h with 160 m<sup>3</sup>/h in average, see Table 1. If the same MVHR uses a membrane moisture recovery heat exchanger (ERV) instead of a heat recovery exchanger (HRV) with the same dimensions (i.e. same volume), the declared heat recovery effectiveness is reduced by about 2 to 9 %-points depending on the volume flow. Correspondingly, applying eq. (3) the measured HR is reduced by about 7 to 14 %-points.

*Table 1: Heat recovery (HR) effectiveness  $\eta_{PHI,declared}$  of HRV and heat and moisture recovery (MR) effectiveness of ERV of different MVHRs ( $\dot{V} < 600$  m<sup>3</sup>/h) according to PHI (passive.de)*

No.	$\dot{V}_{min}$ [m <sup>3</sup> /h]	$\dot{V}_{max}$ [m <sup>3</sup> /h]	HR [%] (HRV)	MR [%] (ERV)	
				HR [%]	MR [%]
1	70	270	90	86	73
2	70	345	88	83	71
3	70	460	87	80	68
4	85	290	86	82	67
5	73	109	89	85	64
6	73	115	89	85	64
7	80	111	86	83	71
8	121	231	93	84	73
9	65	200	87	85	77
10	110	280	83	81	63
11	80	111	86	83	71
12	116	368	90	85	71
13	116	246	92	87	74

## Building Energy and Moisture Balance

### Moisture Balance

Recommended ventilation rates of 20 to 30 m<sup>3</sup>/h/P are a compromise between good indoor air quality (IAQ), acceptable ventilation losses and sufficient relative humidity, which should not fall below 30 %. Thermal comfort can be guaranteed for a wide range of volume flows if a heat recovery ventilation is used. Without MVHR, excessive air exchange rates have to be avoided in order to prevent from cold air down draught.

For a standard occupation density of 30 m<sup>2</sup>/P, a room height of 2.7 m and a ventilation rate of 30 m<sup>3</sup>/h/P, an infiltration rate corresponding to a n<sub>50</sub>-value of 0.6 1/h and a moisture source of  $\dot{S}_v = 100$  g/P/h, the corresponding

indoor air relative humidity can be easily calculated acc. to the steady state moisture balance:

$$\dot{m}_{v,in} - \dot{m}_{v,out} + \dot{S}_v = 0 \quad (4)$$

with the inlet vapour mass flow

$$\dot{m}_{v,in} = \dot{m}_{a,inf} \cdot \omega_{amb} + \dot{m}_{a,vent} \cdot \omega_{sup} \quad (5)$$

and outlet vapour mass flow

$$\dot{m}_{v,out} = (\dot{m}_{a,inf} + \dot{m}_{a,vent}) \cdot \omega_{ext} \quad (6)$$

For an ambient temperature of  $\vartheta_{amb} = 0$  °C with a relative humidity of  $\varphi_{amb} = 80$  % and an extract air temperature of  $\vartheta_{ext} = 22$  °C the corresponding indoor air relative humidity is 33 % assuming an heat recovery effectiveness of  $\eta_T = 82$  %. The supply air temperature is then 19 °C with a rel. humidity of 23 %.

### Moisture equivalent volume flow

Using instead an ERV with a moisture effectiveness of 64 % (for 120 m<sup>3</sup>/h in this example) for the same conditions an indoor relative humidity of 49.7 % could be obtained, see psychrometric diagram, Fig. 2. The ventilation losses (enthalpy difference between extract air and supply air) decrease from 394 W to 356 W. Hence, assuming the same flow rate for HRV and ERV, the indoor (i.e extract) air relative humidity is significantly higher and it is in the comfort zone with ERV. The IAQ would be better with respect to the relative humidity and equal with respect to CO<sub>2</sub>- and/or TVOC-concentration, respectively. (Remark: in this simplified moisture balance, buffer storage effects and the influence of rH on moisture sources are disregarded).

It is difficult to monetarize the better air quality and thermal comfort (i.e. the higher relative humidity). However, instead, we could assume to increase the flow rate such that we obtain equal relative humidity compared to the case without moisture recovery. This “moisture equivalent volume flow” cannot be easily determined as the temperature and moisture effectivenesses change with the volume flow but it has to be determined by means of inverse simulation. To obtain the same indoor air humidity as in case of heat recovery the volume flow can be increased from 120 m<sup>3</sup>/h to 222 m<sup>3</sup>/h. For the same heat exchanger area, the temperature effectiveness decreases by 12 %-points and the moisture transfer effectiveness by 16 %-points (see next section for a detailed description of the model). Hence, the supply air decreases to 16.8 °C with a relative humidity of 34.6 %, see (Fig. 2, right hand side). The ventilation losses increase because of the higher flow rate to 676 W. The additional ventilation losses have to be covered by the heat pump, which will, however, run with better COP.

The IAQ can be improved and due to the higher air flow rate, more energy can be transported with the air (see state sup1, after the condenser) and the efficiency of the exhaust air heat pump can be increased if the same heating power is assumed. There is an additional advantage of significantly reducing the pre-heating energy demand (frost-protection) which has to be considered, see also section “ERV and Exhaust Air Heat Pump”, below.

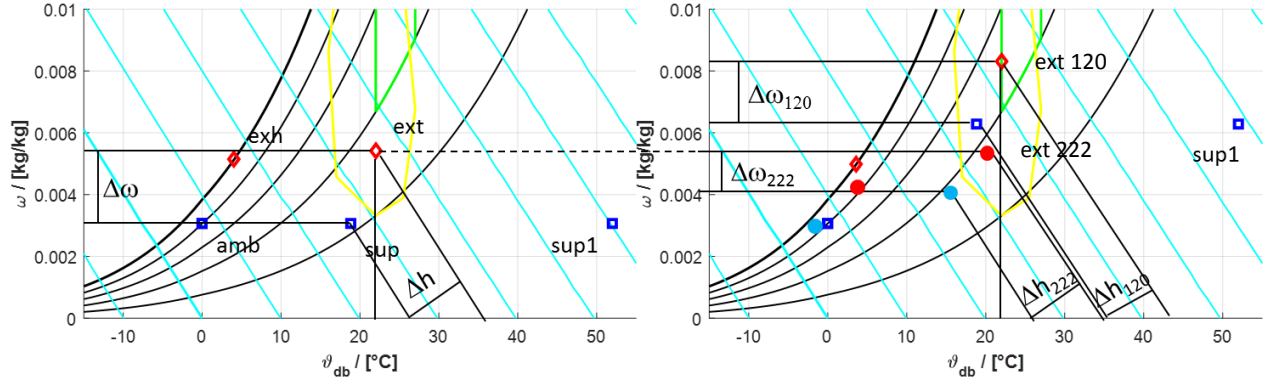


Figure 2: Psychrometric diagram, left hand side: heat recovery with 120 m³/h, right hand side: moisture recovery with 120 m³/h and 222 m³/h, winter case (HR:  $\eta_T = 86\%$  MR w. 120 m³/h:  $\eta_T = 86\%$   $\eta_\omega = 61\%$ , MR w. 222 m³/h:  $\eta_T = 76\%$   $\eta_\omega = 46\%$ ); Humidity ratio difference ( $\Delta\omega$ ) and difference of specific enthalpy related to mass of dry air ( $\Delta h$ ) between extract (ext) air and supply (air), sup1: after condenser of HP

## Modelling ERV

The thermal and hydraulic performance of the cross/counter-flow ERV depends on the boundary conditions (heating or cooling) and operating conditions (volume flow). The quasi-counter-flow arrangement allows to provide relatively high sensible and latent effectiveness. Fluid dynamics may be improved by so-called membrane spacers, which decrease boundary layer thickness introducing turbulences. In particular, the latent effectiveness strongly depends on the relative humidity of the membrane (i.e. the slope of the sorption isotherm) and on the volume flow.

Some authors (such as Niu (2001), Kadylak (2006), Liu et al. (2015)) reported already on modelling and simulation of ERV for either heating or cooling/dehumidification applications. Both, complex numerical models as well as (semi)-empirical models (eta-NTU) have been developed and validated. However, a study in which these approaches are compared, by discussing advantages and limits of each one, is missing until now. Furthermore, an interaction with the building (moisture buffer) has not been sufficiently discussed yet. In the following, both modelling approaches - the fully discrete model and the (semi-) empirical model are presented and discussed. Modelling results are compared with each other and against experimental data from the literature.

### Analytical Model – eta-NTU

The eta-NTU approach is well established in heat exchanger calculation (VDI-HA) and was proposed by some authors (such as Zhang et al. (2002)) for moisture transfer in ERV. For the simple case of a counter flow type heat exchanger with equal mass and capacity flows the sensible and latent effectiveness ( $\eta_T$ ,  $\eta_\omega$ ) can be calculated as follows (see Zhang et al. (2002) or Kadylak (2006) for a more detailed discussion).

$$\eta_{T/(\omega)} = \frac{NTU_{T/(\omega)}}{NTU_{T/(\omega)} + 1} \quad (7)$$

with the number of transfer units (NTU) for heat transfer

$$NTU_T = \frac{A_{eff} \cdot U_T}{\dot{C}} \quad (8)$$

and mass transfer

$$NTU_\omega = \frac{A_{eff} \cdot U_\omega}{\dot{m}_a} \quad (9)$$

The overall heat transfer coefficient  $U_T$  and the overall mass transfer coefficient ( $U_\omega$ ) for the gradient of the humidity ratio ( $\omega$ ) depend on the flow regime and, in case of mass transfer, on the membrane properties, see section below. The thermal conduction resistance of the membrane is usually negligible.

In the majority of cases, capacity flows will not be equal and eq. 7 for the effectiveness has to be replaced by

$$\eta_{counter} = \frac{1 - \exp(-(R_{min} - 1) \cdot NTU_{min})}{1 - R_{min} \cdot \exp(-(R_{min} - 1) \cdot NTU_{min})} \quad (10)$$

with the ratio of the capacity flows  $R_{min}$ . For cross flow heat exchanger the following correlation is suggested in the literature

$$\eta_{cross} = 1 - \exp\left(\frac{\exp(-NTU^{0.78}) - 1}{NTU^{-0.22}}\right) \quad (11)$$

Cross flow effectiveness is – depending on NTU - about 6 to 12.5 % lower than counter flow effectiveness for heat transfer and between 6 % and 9 % lower in case of moisture transfer. In case of mixed counter-cross flow the effectiveness can be weighted by the area.

The eta-NTU method allows to predict the effectiveness based on the properties of the heat/mass exchanger (area  $A$ , membrane properties, see section below) and operation conditions (i.e. volume flow, capacity flow  $\dot{C}$  and mass flow of dry air  $\dot{m}_a$ ). However, the eta-NTU method does not account for the coupling between heat and moisture transfer. The prerequisite for applying the eta-NTU method is a logarithmic mean temperature difference, or a logarithmic mean concentration (or humidity ratio or partial pressure) difference, respectively. For the case of heat transfer, the logarithmic mean temperature difference

applies only in case of dry conditions (no condensation, no mass transfer). The eta-NTU does not allow predicting the effectiveness depending on the boundary conditions and on the mass transfer rate (as discussed in the following sections).

### Numerical Model

Numerical models for heat and mass transfer were discussed already in the literature (see e.g. Zhang et al. (1999), Jingchun et al. (2011), Yaici et al. (2013)). For cross flow ERVs, 2D models are required. 3D models are usually not necessary as the conduction/diffusion in the membrane in the direction of the flow can be disregarded (see Zhang et al. (1999)).

For the simple case of a counter flow heat exchanger, the following system of non-linear equations, which is exemplarily given for stream 1 has to be solved.

Energy Balance

$$\begin{aligned} c_{p,a} \cdot \vartheta_{1,j} + \min(\omega_j, \omega'_j) \cdot (c_{p,v} \cdot \vartheta_{1,j} + \Delta h_v) \\ = c_{p,a} \cdot \vartheta_{1,j+1} + \min(\omega_{j+1}, \omega'_{j+1}) \\ \cdot (c_{p,v} \cdot \vartheta_{1,j+1} + \Delta h_v) + \frac{U_T A_{eff}}{\dot{m}_{a,1}} \cdot (\vartheta_{1,j} - \vartheta_{2,j}) \end{aligned} \quad (12)$$

Mass Balance

$$\omega_{1,j} = \omega_{1,j+1} + \frac{U_{m,\omega} A_{eff}}{\dot{m}_{a,1}} \cdot d\omega_v \quad (13)$$

In equations (12) and (13),  $\vartheta$  is the temperature,  $\omega$  is the humidity ratio,  $\omega'$  is the humidity ratio at saturation,  $c_p$  is the specific heat capacity at constant pressure for air (a) and vapour (v),  $\Delta h_v$  is the latent heat of vaporization and  $\dot{m}_{a,1}$  is the mass flow of dry air of stream 1. The overall heat ( $U_T$ ) and moisture ( $U_{m,\omega}$ ) transfer coefficients are discussed in detail in the following sections.

The *fsolve* function in Matlab is used to solve the system of N times 2 (streams) times 2 (mass and energy balance) non-linear equations with N denoting the number of segments. The boundary conditions are the temperature and humidity ratio at both inlets (i.e. extract air and ambient air). It was found that at least  $N > 150$  nodes are required to get sufficiently accurate results.

## ERV – heat and mass transfer

### Overall heat and mass transfer coefficient

The heat flux  $\dot{Q}$  transferred in the heat exchanger is proportional to the area A, the overall heat transfer coefficient U and the logarithmic temperature difference  $\Delta\vartheta_{log}$ .

$$\dot{Q} = U_T A \cdot \Psi \cdot \Delta\vartheta_{log} \quad (14)$$

Correspondingly, the mass transfer  $\dot{m}_v$  can be calculated with the overall mass transfer coefficient  $U_{m,p}$  and the logarithmic partial pressure difference.

$$\dot{m}_v = U_{m,p} A \cdot \Psi_m \cdot \Delta p_{v,log} \quad (15)$$

$\Psi$  is a correction factor, which is smaller than one, if heat and mass transfer is different to the ideal case of counter

flow (e.g. in cross flow or in the case condensation occurs).

The overall heat transfer coefficient is

$$U_T = \frac{1}{\frac{1}{\alpha} + \frac{d}{\lambda} + \frac{1}{\alpha}} \quad (16)$$

The conduction resistance of the membrane  $d/\lambda$  is usually negligible compared to the convective heat transfer coefficient  $\alpha$ .

The overall mass transfer coefficient related to concentration gradient  $U_c$  is a function of the mass transfer coefficient  $\beta$  and the diffusion resistance of the membrane  $d_{mem}/D_{mem}$ .

$$U_c = \frac{1}{\frac{1}{\beta} + \frac{d_{mem}}{D_{mem}} + \frac{1}{\beta}} \quad (17)$$

The overall mass transfer coefficient can also be defined for the gradient of the humidity ratio ( $U_\omega$ ) and for the vapour pressure gradient ( $U_p$ ), while

$$U_\omega = U_c \frac{M_a \cdot c_m}{x_{a,m}} \quad (18)$$

and

$$U_p = U_c \cdot R_v \cdot T \quad (19)$$

In eqs. (18) and (19)  $R_v$  is the individual gas constant of water,  $M_a$  the molar mass of air,  $c_m$  the mean molar concentration and  $x_{a,m}$  the logarithmic mean molar fraction of air, which depends on the humidity ratio  $\omega$ .

### Heat and Mass Transfer Coefficient

The heat transfer coefficient  $\alpha$  can be calculated using well known Nusselt (Nu) correlations with the thermal conductivity ( $\lambda$ ) of the air and the hydraulic diameter (dh).

$$\alpha = \frac{Nu \cdot \lambda}{dh} \quad (20)$$

The flow through the heat exchanger can be assumed to be laminar for all relevant volume flows because of the narrow space in the channels. For heat transfer in rectangular channels some authors suggest the following Nu-correlation, which applies for fully developed flow

$$Nu = -7.4818 \cdot a_r^3 + 18.535 \cdot a_r^2 - 15.663 \cdot a_r + 8.235 \quad (21)$$

with the aspect ratio  $a_r$ .

$$a_r = \frac{height}{width} \quad (22)$$

Other authors, e.g. Zhang et al. (1999) suggest Nu as a function of Reynolds (Re) and Prandtl (Pr) number such as:

$$\begin{aligned} Nu \\ = 3.658 + \frac{0.085 \cdot \left( Re Pr \frac{dh}{L} \right)}{1 + 0.047 \cdot \left( Re Pr \frac{dh}{L} \right)^{.67}} \left( \frac{\eta_b}{\eta_s} \right)^{.14} \end{aligned} \quad (23)$$

or

$$Nu = 1.86 \left( Re \cdot Pr \cdot \left( \frac{d_h}{L} \right) \right)^{.33} \cdot \left( \frac{\eta_b}{\eta_s} \right)^{.14} \quad (24)$$

Nu depends on the hydraulic diameter  $d_h$  and the length of the channel  $L$ . The ratio of the dynamic viscosity of the bulk  $b$  and the surface  $s$  ( $\eta_b/\eta_s$ )<sup>.14</sup> can be disregarded here, because of the low temperature differences. With equations (23) and (24) the convective heat transfer coefficient is in the range of 20 W/(m<sup>2</sup> K).

With equation (21) the convective heat transfer coefficient takes values between 35.1 W/(m<sup>2</sup> K) for an aspect ratio of 1 and 39.9 W/(m<sup>2</sup> K) for the actual aspect ratio of 0.041 independent of the flow rate and assuming fully developed flow. Gendebien et al. (2013) used correlations given in Nellis et al. (2009), which use corrections to consider the entrance region. For the considered example (Zhong et al. (2014), see below), with a cross section of the heat exchanger of 0.182 m x 0.462 m, a channel width of 2.5 mm, a membrane thickness of 75  $\mu$ m and 90 channels, the convective heat transfer coefficient increases from 39.6 W/(m<sup>2</sup> K) to 41.2 W/(m<sup>2</sup> K) if the flow rate increases from 100 to 200 m<sup>3</sup>/h.

Heat and mass transfer coefficients are correlated, as shown by many authors. The well-known Lewis correlation is

$$\beta = \frac{\alpha}{\rho_a c_{p,a}} \cdot Le^{-2/3} \quad (25)$$

The Lewis number

$$Le = \frac{\lambda_a}{\rho_a c_{p,a} \cdot D_v} \quad (26)$$

is usually given with  $Le = 0.87$  for these kind of applications.

### Membrane properties: diffusion through a membrane

Vapor diffusion through a membrane can be described by the first Fickian law which can be formulated as.

$$\dot{m}_v = \frac{D_v}{R_v \cdot T \cdot d_{mem} \cdot \mu} \cdot \Delta p_v \quad (27)$$

The equivalent air layer thickness  $s_d$  is the product of the membrane thickness  $d_{mem}$  and the water vapour diffusion resistance factor  $\mu$ , which is a material property and depends on the relative humidity  $\phi$  as discussed in the following.

$$s_d = \mu \cdot d_{mem} \quad (28)$$

In previous studies (e.g. Liu et al. 2015) the humidity dependence of the vapour diffusion resistance factor  $\mu$  was mentioned, but usually it is disregarded.

The vapour diffusion resistance factor  $\mu$  decreases with the moisture content of the membrane  $u$ .

$$\mu = \frac{D_v}{D_{mem} \cdot \frac{du}{d\phi} \cdot \frac{p}{p_s}} \cdot \frac{M_v \cdot c_m}{x_{a,m}} \quad (29)$$

$D_v$  is the diffusion coefficient of moisture in air

$$D_v = 22.2E - 6 \cdot \left( \frac{1E5}{p} \right) \cdot \left( \frac{T_m}{273.15} \right)^{1.81} \quad (30)$$

and  $D_{mem}$  the diffusion coefficient of the membrane, which has to be determined by experiments. The saturation pressure  $p_s$  can be approximated e.g.

$$p_s = 1.629E11 \cdot \exp \left( -\frac{5294}{T} \right) \quad (31)$$

$p$  is the absolute pressure,  $M_v$  the molar mass,  $c_m$  the mean molar concentration and  $x_{a,m}$  the logarithmic mean molar fraction of air, which depends on the humidity ratio  $\omega$  (Niu et al. (2001)).

The moisture content of the membrane  $u$  is a function of the relative humidity and can be described with the sorption isotherm. A relative simple approach is given in e.g. Alonso et al. (2015):

$$u = \frac{u_{max}}{1 - C + \frac{C}{\phi}} \quad (32)$$

Then the derivative with respect to the rel. humidity is

$$\frac{du}{d\phi} = \frac{C \cdot u_{max}}{\left( 1 - C + \frac{C}{\phi} \right)^2 \cdot \phi^2} \quad (33)$$

The coefficient  $C$  is a material property, which has to be determined by means of measurements. This rather simple approach for the dependence of the water vapour diffusion resistance factor on the membrane relative humidity on is shown in Fig. 3. Authors report about a wide range of the coefficient  $C$ , which is as low as 2 (Liu et al. (2015)), 10 (Aarnes (2012)) or 184 (Kadylak (2006)).

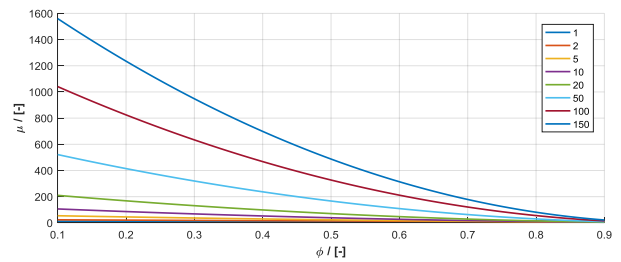


Figure 3: Water vapour diffusion resistance factor  $\mu$  (top) as a function of the relative humidity with the fitting coefficient  $C$  as parameter;  $u_{max} = 0.23$  kg/kg;  $d_{mem} = 0.032E-3$  m;  $D_{mem} = 7.5E-8$  kg(m s);

### Experimental Validation

In the literature, experimental data is available for the membrane only, i.e. for the  $s_d$ -value e.g. in Min et al. (2011) and for different configurations of the air-to-air heat exchanger e.g. Zhang (2010), Liang (2014), Zhong et al. (2014), Liu et al. (2016). For the validation of the above presented models experimental data reported in the literature is taken.

For a given geometry and applying the correlations for convective heat transfer coefficient given above, in order to calibrate the analytical or the numerical model, only two fitting parameters remain unknown: the effective heat exchanger area  $A_{eff}$  and the water vapour diffusion



resistance factor  $\mu$ . Contrariwise, if the flow regime is not predictable with sufficient accuracy, the effective heat transfer capability  $U \cdot A_{\text{eff}}$  and the effective moisture transfer capability  $A_{\text{eff}}/\mu$  can be used as fitting parameters.

Three exemplary cases are considered: Liu et al. (2016) present measured data of a relative small functional model of a quasi-counter flow heat exchanger for winter conditions (ext: 21 °C, 40 %). Zhong (2014) presents a wide range of experimental results for a 0.182 m x 0.182 m x 0.462 m cross flow heat exchanger configuration including different membranes and different structures for summer conditions (ext: 27 °C, 50 % amb: 35 °C, 70 %). Two examples out of six are considered here.

The sensible and latent effectiveness is shown as a function of the volume flow in Fig. 4. Data from Liu et al. (2016) is compared against the results of the eta-NTU method and of the numerical model, described above.

With both methods, relative good agreement can be obtained and the trends can be predicted well. The flow rate influences both, the temperature effectiveness and the moisture effectiveness  $\eta_{\omega}$ , and has a major impact on the latter. If the flow rate is doubled, e.g. from 30 m<sup>3</sup>/h to 60 m<sup>3</sup>/h the sensible effectiveness decreases from 90 % to 85 %, while the latent effectiveness decreases from 72 % to 58 %.

The experimental results can be predicted with both, the analytical (eta-NTU) and the numerical model rather well in case of quasi-counter flow configuration. With the eta-NTU method, better agreement between measured and calculated data can be obtained assuming 40 % cross and 60 % counter flow with an effective area of  $A_{\text{eff}} = 10 \text{ m}^2$  and a water vapour diffusion resistance of  $\mu = 175$  as shown in Fig. 5.

The comparison of experimental data (from Zhong et al. (2014)) with simulated data for the summer case is shown in Fig. 6 and Fig. 7 for two cases with different plate type membrane heat exchangers. Because of the cross flow configuration, the 1D discrete model is not able to predict the effectiveness very well: the decrease of the effectiveness with the volume flow is overestimated. The eta-NTU model delivers similar results for the latent effectiveness, but it completely overestimates the sensible heat transfer as the influence of latent on sensible heat transfer is not considered ( $\eta_T$  calculated with the eta-NTU approach is not shown in Fig. 6 and 7). This effect is much more pronounced in summer conditions, where the temperature differences are generally lower (e.g. 35 °C-27 °C = 8 K instead of 21 °C – 0 °C = 21 K).

The numerical model and the experimental data agree quite well for the temperature effectiveness in case of membrane “C”, but there are relative large deviations in case of type “E” in particular for low volume flows.

Effectivenesses shown in Fig. 4 and 5 are related to the extract-exhaust air ( $\eta_{T1}$ ,  $\eta_{\omega 1}$ ). In Fig. 6 and 7 the effectiveness is the average between exhaust and extract air ( $\eta_{T/\omega,1}$ ) and ambient and supply air ( $\eta_{T/\omega,2}$ )

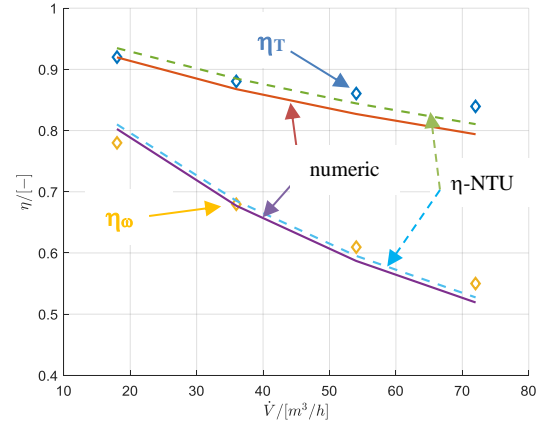


Figure 4: Sensible and latent effectiveness (marker, acc. to Liu et al. (2016)); calculated (dashed line, eta-NTU) and simulated (solid line) effectiveness as a function of the volume flow;  $A_{\text{eff}} = 6 \text{ m}^2$ ,  $\mu = 175$ ;  $\eta_T = (\vartheta_{\text{ext}} - \vartheta_{\text{exh}}) / (\vartheta_{\text{ext}} - \vartheta_{\text{amb}})$ ,  $\eta_{\omega} = (\omega_{\text{ext}} - \omega_{\text{exh}}) / (\omega_{\text{ext}} - \omega_{\text{amb}})$

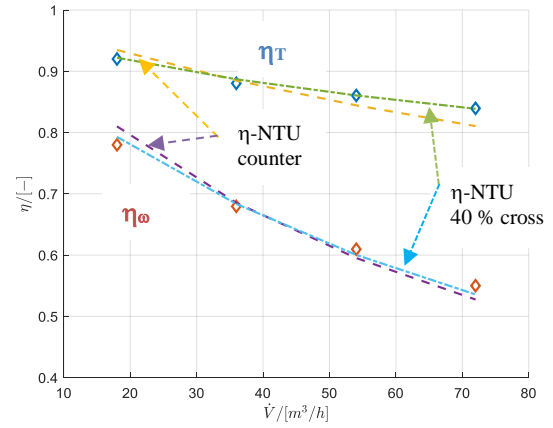


Figure 5: Sensible and latent effectiveness as a function of the volume flow; measured (marker, acc. to Liu et al. (2016)) and calculated with eta-NTU (dashed line, counter-flow and dash-dotted line 40 cross flow);  $A_{\text{eff}} = 10 \text{ m}^2$ ,  $\mu = 250$ ;  $\eta_{T/\omega}$  as in Fig. 4.

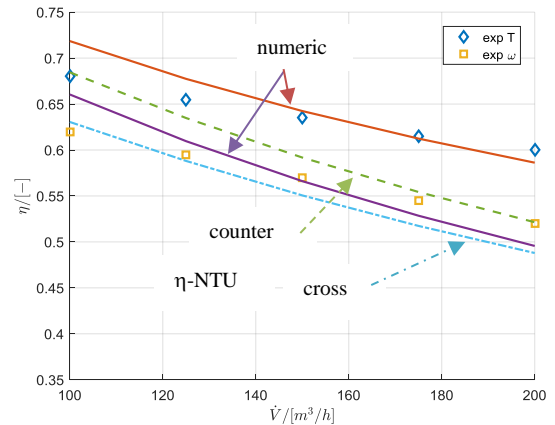


Figure 6: Sensible and latent measured (marker, acc. to Zhong et al. (2014) “type E”) and simulated effectiveness for a plate type heat exchanger in cross flow configuration; (solid line, simulation), dashed and dashed-dotted line eta-NTU;  $A = 22.5 \text{ m}^2$ ,  $\mu = 125$ ; here: average effectiveness of both streams  $\eta_{T/\omega} = (\eta_{T/\omega,1} + \eta_{T/\omega,2}) / 2$

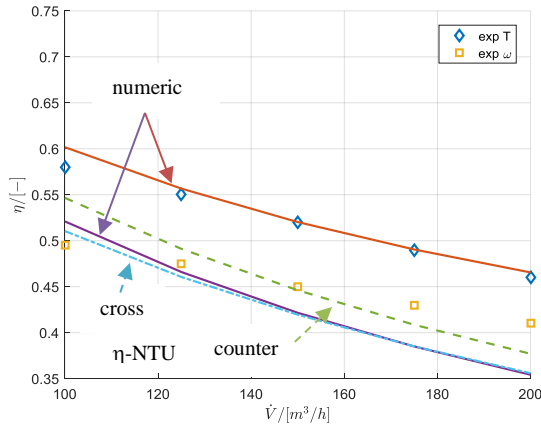


Figure 7: Sensible and latent measured (marker, acc. to Zhong et al. (2014) “type C”) and simulated effectiveness for a plate type heat exchanger in cross flow configuration; (solid line, simulation), dashed and dashed-dotted line eta-NTU;  $A = 12.5$ ,  $\mu = 125$  here: average effectiveness of both streams  

$$\eta_{T/\omega} = (\eta_{T/\omega,1} + \eta_{T/\omega,2})/2$$

It has to be noted here again, that the eta-NTU model cannot predict the influence of the moisture transfer on the heat transfer, i.e. if due to the moisture transfer or because of condensation, the temperatures of supply and exhaust air are substantially influenced, the temperature effectiveness can not be predicted accurately with the eta-NTU approach.

The numerical model and the eta-NTU model are in good agreement for the moisture effectiveness of the entire range of the considered water vapour diffusion resistance factor and for both, the winter (0 °C, 80 %, 22 °C 50 %) and the summer case (35 °C, 80 %, 26 °C 50 %). The effect that the temperature effectiveness increases with increasing water vapour diffusion resistance factor because of the coupled heat and mass transfer, can be predicted with the numerical model, but is disregarded by the eta-NTU approach.

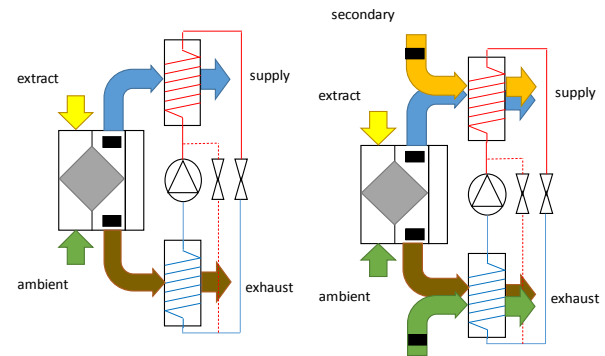
## ERV and Exhaust Air Heat Pump

### Concepts for Exhaust Air Heat Pumps

Heating of a house with very low heating demand and very low heat load can be done with a Passive House compact heat pump with air heating – usually with an exhaust air heat pump. A combination of membrane ERV and exhaust air heat pump (as e.g. in so-called compact units for Passive Houses) was not discussed in any of the previous studies.

An exhaust air heat pump (EAHP) extracts heat from the exhaust air of a building and transfers the heat typically to the supply air. But also variants with hydronic heating system (floor heating, radiators) and DHW preparation exist. State of the art compact units (e.g. PKom4 from the company Pichler Luft) allow additionally for some supply-air cooling, but still there is no experience on how ERV influences the performance in heating mode or under cooling conditions.

This type of heat pump works in combination with a MVHR and its output power is coupled to the hygienic air flow rate (e.g. 120 m³/h). The sink can be either the supply air (air heating system), a buffer storage (in a hydronic heating system) or both. The inside air temperature is approximately 20 to 22 °C all over the heating period and the MVHR damps the influence of the ambient temperature. Therefore, the output power of the heat pump is not varying much with the seasons and outdoor temperature. Newer versions suck additional ambient air through the evaporator to increase the power in times of high heating loads and usually work with an inverter controlled compressor. Furthermore, secondary air (i.e. recirculated air from overflow zones, e.g. the corridor) can be used to increase the maximum heating capacity in case of air heating, see Fig. 9, right hand side. Heating power of the heat pump can vary from about 1 kW to 6 kW.



MVHR with exhaust air heat pump limited to 10 W/m²

MVHR with exhaust air heat pump with secondary air and ambient air for heating power higher than 10 W/m²

Figure 9: Concepts of exhaust air heat pumps (Ochs et al. 2017), MVHR with or without moisture recovery

As the exhaust air as source for an air-to-air heat pump, the performance of the heat pump is directly connected to the performance of the ERV. In case of air heating, the performance of the heat pump depends on both, exhaust air temperature/enthalpy and supply air temperature, which are both influenced by the effectiveness of the ERV.

### Performance of exhaust air HP with HRV and ERV

Different exhaust air HP concepts are compared by means of steady-state simulation with a simplified physical HP model (developed in Matlab using CoolProp). The objective is to investigate the influence of moisture recovery on the HP and system performance for different operation conditions. The simulations are performed for the following boundary conditions and the parameters listed in Table 2:

- Ambient air temperature -8°C; Ambient air relative humidity 80 %
- Indoor air temperature +22 °C; Indoor air relative humidity 30 %

- Pre-heating of ambient air to 0 °C (no pre-heating in case of moisture recovery); remark: the set point for defrosting has high influence on the electricity consumption; usually set point some degree below 0 °C is possible.
- Max. supply air temperature +52 °C (reference)

Table 2: Parameter for the simplified physical MHVR and HP model

Parameter	Formula	Value	Unit
Specific fan power	SFP <sub>MVHR,fan</sub>	0.2	Wh/m <sup>3</sup>
	SFP <sub>amb</sub>	0.06	Wh/m <sup>3</sup>
	SFP <sub>sec</sub>	0.1	Wh/m <sup>3</sup>
Heat exchanger area	A <sub>HX</sub>	17.5	m <sup>2</sup>
Water vapour diffusion resistance factor	μ	300	-
Pre-heating	θ <sub>lim</sub>	0	°C
Refrigerant	R	R134a	-
Sub-cooling	ΔT <sub>sub</sub>	5	K
Super-heating	ΔT <sub>sup</sub>	5	K
Temperature difference evaporator	ΔT <sub>evap</sub>	3	K
Temperature difference condenser	ΔT <sub>cond</sub>	3	K
Electric efficiency	η <sub>el</sub>	0.85	-
Isentropic efficiency τ = P <sub>cond</sub> /P <sub>evap</sub> (compression ratio)	η <sub>is</sub>	0.82 (τ=4)	-
		0.75 (τ=8)	-
		0.75 (τ=2)	-

The simplifying assumptions for this comparison are that ERV and HRV have equal heat exchanger area and that for all conditions the compressor can be controlled such that the exhaust air heat pump delivers for all configurations and operation conditions the same heating power. In case of higher flow rates, the HP covers the additional ventilation losses.

By means of inverse simulation, for each concept the electric power of the compressor is determined such that the heating power is equal for all concepts. For sake of simplicity it is assumed that the compressor can be operated within the considered power range with an electric efficiency of 80 % and a typical isentropic efficiency as a function of the compression ratio as indicated in Table 2. Then the performance of the

concepts is calculated and compared. The simulated performances of the different configurations of exhaust air HPs are summarized in Table 3 and 4. The COPs are calculated as shown in equations (34) to (40).

MVHR:

$$COP_{MVHR} = \frac{\dot{Q}_{MVHR}}{P_{el,fan}} \quad (34)$$

$$COP_{MVHR,sys} = \frac{\dot{Q}_{MVHR} + \dot{Q}_{pre-heat}}{P_{el,fan} + \dot{Q}_{pre-heat}} \quad (35)$$

Exhaust air HP:

$$COP_{REF} = \frac{h_2 - h_3}{h_2 - h_1} \quad (36)$$

$$COP_{HP} = \frac{\dot{Q}_{cond}}{P_{el,comp}} \quad (37)$$

$$COP_{SYS} = \frac{\dot{Q}_{cond} + \dot{Q}_{MVHR} + \dot{Q}_{pre-heat} + \dot{Q}_{post-heat}}{P_{el,MVHR} + P_{el,comp} + \dot{Q}_{pre-heat} + \dot{Q}_{post-heat}} \quad (38)$$

Exhaust air HP w\ secondary and additional ambient air:

$$COP_{HP} = \frac{\dot{Q}_{cond}}{P_{el,comp} + P_{el,fan}} \quad (39)$$

$$COP_{SYS} = \frac{\dot{Q}_{cond} + \dot{Q}_{MVHR} + \dot{Q}_{pre-h.} + \dot{Q}_{post-h.}}{P_{el,MV.} + P_{el.co.} + P_{el,fan} + \dot{Q}_{pre-h.} + \dot{Q}_{post-h.}} \quad (40)$$

Exemplarily, the refrigerant cycle is shown for the cycle with 120 m<sup>3</sup>/h of hygienic air exchange, 120 m<sup>3</sup>/h of additional ambient air and 120 m<sup>3</sup>/h of secondary air with heat recovery and with moisture recovery in Fig. 10.

As can be seen in Table 3, with moisture recovery and with equal flow rate (of here 120 m<sup>3</sup>/h), the performance of the heat pump decreases (here from 2.5 to 2.3) because of the lower enthalpy remaining in the exhaust air after the MVHR. There is still an increase of the system performance as the COP of the MVHR is significantly better in case of moisture recovery because the pre-heating can be avoided.



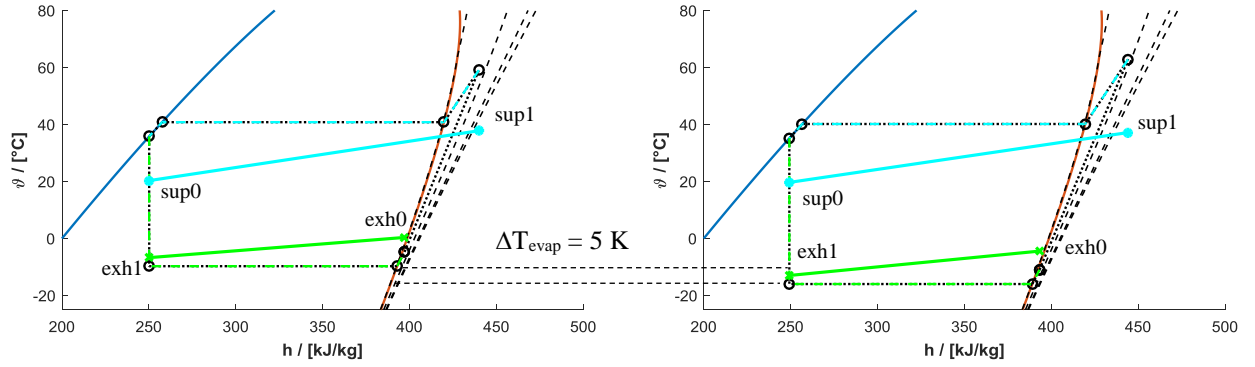


Figure 10: Temperature-enthalpy diagram (R134a) for the case with heat recovery (left) and moisture recovery (right) for 120 m³/h hygienic air exchange, 120 m³/h additional ambient air and 120 m³/h secondary air; sup0 after MVHR, before condenser, sup1 after condenser, exh0 after MFHR before evaporator, exh1 after evaporator

As discussed in the previous sections, with moisture recovery, the hygienic air exchange rate can be increased without violating the lower recommended boundary of the relative humidity (usually 30 %). The moisture equivalent volume flow with moisture recovery is 222 m³/h compared to 120 m³/h.

Table 3: Results for the exhaust air heat pump (see Fig. 2 left hand side) for heat recovery (HR) with a volume flow of 120 m³/h and with moisture recovery (MR) with 120, 150 and 222 m³/h;  $\dot{Q}_{MVHR}$  heat flux transferred by MVHR,  $\dot{Q}_{pre-heat}$  heat flux for frost-protection,  $\dot{Q}_{HP}$ : Heat flux delivered by HP (condenser),  $\dot{Q}_{loss,comp}$ : thermal losses of compressor,  $\dot{H}_{ext} - \dot{H}_{sup}$ : ventilation losses,  $COP_{ref}$ : COP of refrigerant cycle (based on specific enthalpies)

Quantity	Unit	HR 120	MR 120	MR 150	MR 222
$rH_{ext}$	[-]	0.30	0.55	0.44	0.30
$\vartheta_{sup}$	[°C]	18.8	17.6	16.7	14.7
$rH_{sup}$	[-]	0.11	0.48	0.39	0.30
$\eta_{T1}$	[-]	0.85	0.85	0.82	0.76
$\eta_{w1}$	[-]	0.00	0.60	0.55	0.45
$\eta_{T2}$	[-]	0.85	0.85	0.82	0.76
$\eta_{w2}$	[-]	0.00	0.60	0.55	0.45
$\dot{Q}_{MVHR}$	[W]	1359	1632	1790	2172
$\dot{Q}_{pre-heat}$	[W]	352	0	0.0	0.0
$\dot{H}_{ext} - \dot{H}_{sup}$	[W]	525	532	657.4	980.1
$\vartheta_{sup1}$	[°C]	52.0	50.7	45.5	38.2
$\dot{Q}_{HP}$	[W]	1466	1472	1597	1920
$\dot{Q}_{loss,comp}$	[W]	81	90	86.0	84.7
$COP_{MVHR,sys}$	[-]	2.9	34.0	29.8	24.5
$COP_{ref}$	[-]	2.7	2.5	2.8	3.4
$COP_{HP}$	[-]	2.5	2.3	2.5	2.9
$COP_{sys}$	[-]	2.8	4.5	5.4	6.3

The COP of the exhaust air HP can be increased from 2.5 (HR), or 2.3 (MR) at 120 m³/h to 2.9 at 222 m³/h.

If instead additional ambient air is used as source and secondary air is used additionally in the condenser, the COP can be improved from 2.5 to 3.1 in case of heat recovery and from 2.3 to 2.9 in case of moisture recovery. The improvement is less pronounced in case of higher air flow rates, but with 8.9 % still relevant.

The maximum possible heating power can be improved with both measures, moisture recovery and secondary air, as can be seen from the supply air 1 in Table 3 and 4 (remark: max. air temperature should not exceed 52 °C).

Table 4: Results for the exhaust air heat pump with 120 m³/h recirculation and 120 m³/h additional ambient air (see Fig. 2, right hand side) and comparison with results acc. to Table 3.

Quantity	Unit	HR 120	MR 120	MR 150	MR 222
$\vartheta_{sup1}$	[°C]	37.7	37.2	35.7	32.9
$\dot{Q}_{HP}$	[W]	1466	1472	1597	1921
$\dot{Q}_{loss,comp}$	[W]	61	65	67.1	73.8
$COP_{MVHR,sys}$	[-]	2.9	34.0	29.8	24.5
$COP_{ref}$	[-]	3.6	3.4	3.6	3.9
$COP_{HP}$	[-]	3.1	2.9	3.0	3.2
$COP_{sys}$	[-]	3.2	6.2	6.4	6.8
Rel. $COP_{HP}$	[%]	24.6	29.6	20.3	8.9
Rel. $COP_{sys}$	[%]	13.9	38.7	20.2	8.9

## Conclusion

Particularly in combination with an exhaust air heat pump, giving a recommendation of whether or not to use a membrane ERV is not easily possible because of the complex relations. The effectiveness cannot be used as single decisive indicator. Moisture recovery allows increasing the volume flow without violating the recommended lower limit for indoor humidity. With higher volume flow, IAQ can be improved and the

performance of an exhaust air heat pump can be enhanced. The presented results represent one working point. Detailed building and system simulation are required to determine the economic feasibility of moisture recovery depending on the operation and boundary conditions such as climate and occupation (i.e. internal heat and moisture gains) profile.

Both models, the eta-NTU and the numerical model, predict the influence of the volume flow rather well for the winter case. In summer, the eta-NTU approach overestimates the temperature effectiveness by far, as the coupling of the heat and moisture transfer mechanisms are not accounted for. The numerical model has to be used here instead. However, there is need for improvement with respect to mixed cross/counter flow configurations and with respect to the convective heat transfer coefficient and the membrane properties. The dependence of the average rel. humidity on the water vapour diffusion resistance factor cannot be directly recognised from the considered cases. The mass transfer potential of different membranes taken from the literature, e.g. Kadylak (2006) does not correspond to the ones identified by the inverse simulation. Further experimental work is required and will be done with the newly developed test stand for ERV and compact units: Within the Austrian FFG project “SaLüH!” measurements of the effectiveness of ERVs and the influence on the performance of the exhaust air heat pump will be performed for different boundary conditions in the near future.

Future work must also focus an air distribution with a transient multi-zone approach including moisture buffer.

## Acknowledgement

This work is part of the Austrian research project SaLüH! Renovation of multi-family houses with small apartments, low-cost technical solutions for ventilation, heating & hot water (2015-18); Förderprogramm Stadt der Zukunft, FFG, Project number: 850085.

## References

Aarnes SM. Membrane based heat exchanger. (M.Sc. Thesis in Product Design and Manufacturing, Department of Energy and Process Engineering). Norway: Norwegian University of Science and Technology; 2012

Alonso, M. J., Peng Liu, Martin H. M. Gaoming G., Simonson C. (2015), Review of heat/energy recovery exchangers for use in ZEBs in cold climate countries. *Building and Environment*. vol. 84, 2015.

Gendebien S., Bertagnolio S., Lemort V. (2013), Investigation on a ventilation heat recovery exchanger: Modeling and experimental validation in dry and partially wet conditions, *Energy and Buildings*, Vol 2, p176-189, Elsevier, 2013.

Kadylak D. E. (2006), Effectiveness Method for Heat and Mass Transfer in Membrane Humidifiers, 2006.

Liang Caihang, (2014), Research on a Refrigeration Dehumidification System with Membrane-Based Total Heat Recovery, *Heat Transfer Engineering*, Taylor and Francis, 2014.

Liu P., Alonso M.J., Martin, H. (2015), Membrane Energy Exchanger, Evaluation of a frost-free design and its performance for ventilation in cold climates, *Proceedings of the 24th International Congress of Refrigeration*, 2015.

Liu P., Alonso M.J., Mathisen, HM Simonson C. (2016), gPerformance of a quasi-counter-flow air-to-air membrane energyexchanger in cold climates, *Energy and Buildings* 119 (2016) 129–142.

Min Jingchun, Hu Teng, Song Yaozu (2011), Experimental and numerical investigations of moisture permeation through membranes, *Journal of Membrane Science*, Volume 367, Issues 1–2, 1 February 2011, Pages 174–181.

Nellis G.F., Klein S.A., (2009) *Heat Transfer*, Cambridge University Press, 2009, Section 5.2.4.

Niu J. L. , Zhang L. Z. (2001), “Membrane-based enthalpy exchanger: material considerations and clarification of moisture resistance,” *Journal of membrane science*, vol. 189, pp. 179–191, 2001.

Ochs F., Pfluger R., Dermentzis G., Siegele D., (2017) *Energy Efficient Renovation with Decentral Compact, Heat Pumps*, 12<sup>th</sup> IEA Heat Pump Conference 2017, Rotterdam.

Schnieders J., Pfluger R., Feist W. (2008), *Energetische Bewertung von Wohnungslüftungsgeräten mit Feuchterückgewinnung*. Passivhaus Institut, Darmstadt, 2008.

Wahiba Yaïci, Mohamed Ghorab, Evgueniy Entchev (2013), Numerical analysis of heat and energy recovery ventilators performance based on CFD for detailed design, *Applied Thermal Engineering* 51 (2013) 770e780.

Zhang, L.-Z. Jiang Y. (1999), Heat and mass transfer in a membrane-based energy recovery ventilator, *Journal of Membrane Science*, Volume 163, Issue 1, 1 October 1999, Pages 29–38.

Zhang L. Z., Niu J. L., (2002), Effectiveness correlations for heat and moisture transfer processes in an enthalpy exchanger with membrane cores, *Journal of Heat Transfer*, vol. 124, pp. 922–929, October 2002.

Zhang, L.-Z. (2010), Heat and mass transfer in a quasi-counter flow membrane-based total heat exchanger. *International Journal of Heat and Mass Transfer* 53(23-24): 5478-5486.

Zhong Ting-Shu, Li Zhen-Xing, Zhang Li-Zhi (2014) Investigation of Membrane-Based Total Heat Exchangers with Different Structures and Materials, *Journal of Membrane and Separation Technology*, 2014, 3, 1-10.

CoolProp: <http://www.coolprop.org/> (visited 2016)